

Microtubule-dependent transport of secretory vesicles visualized in real time with a GFP-tagged secretory protein

Irene Wacker^{1,*}, Christoph Kaether^{2,*}, Andreas Krömer², Andrea Migala¹, Wolf Almers¹ and Hans-Hermann Gerdes^{2,†}

¹MPI for Medical Research, Jahnstrasse 29, 69120 Heidelberg, Germany

²Department of Neurobiology, University of Heidelberg, Im Neuenheimer Feld 364, 69120 Heidelberg, Germany

*Both these authors contributed equally to this work

†Author for correspondence (e-mail: hhgerdes@sun0.urz.uni-heidelberg.de)

SUMMARY

Biosynthetic transport from the *trans*-Golgi network (TGN) to the plasma membrane (PM) is mediated by secretory vesicles. We analyzed secretory vesicle transport in real time using a GFP-tagged secretory protein, hCgB-GFP, consisting of human chromogranin B (hCgB) and green fluorescent protein (GFP). The fusion protein was expressed transiently in Vero cells or in a stable clone after induction with butyrate. After arrest of the biosynthetic protein transport at 20°C, fluorescent hCgB-GFP colocalized with TGN38, a marker of the TGN. Subsequent release of the secretion block at 37°C led to the formation of green fluorescent vesicles. Confocal analysis revealed that these vesicles were devoid of TGN38 and of Texas Red-coupled transferrin and cathepsin D, markers of the endosomal/lysosomal pathway. As determined by fluorometry and metabolic labelling hCgB-GFP was secreted from the TGN to the PM with a $t_{1/2}$ of 20-30 minutes. Video-

microscope analysis of green fluorescent vesicles showed brief periods of rapid directed movement with maximal velocities of 1 $\mu\text{m}/\text{second}$. Vesicle movement occurred in all directions, centrifugal, centripetal and circumferential, and 50% of the vesicles analyzed reversed their direction of movement at least once within an observation period of 45 seconds. In the presence of nocodazole the movement of fluorescent vesicles ceased. Concomitantly, secretion of hCgB-GFP was slowed but not completely blocked. We suggest that microtubules (MT) facilitate the delivery of secretory vesicles to the PM by a stochastic transport, thereby increasing the probability for a vesicle/target membrane encounter.

Key words: GFP, TGN, Real time, Secretory vesicle, Microtubule, Chromogranin B

INTRODUCTION

The biosynthetic pathway in mammalian cells consists of the endoplasmic reticulum (ER) and the various compartments of the Golgi-complex, and is spatially organized and held in place by microtubules (MT) (Cole and Lippincott-Schwartz, 1995; Kelly, 1990; Schroer and Sheetz, 1991). In nonpolarized cells MT radiate from a perinuclear MT-organizing center (MTOC) to the cell periphery. While the ER is distributed throughout the cell the Golgi complex is centrally located near the MTOC. MT do not only provide a static scaffold for the positioning of the biosynthetic compartments but also mediate dynamic interactions between them (Cole and Lippincott-Schwartz, 1995). Disassembly of the microtubules disrupts the spatial organization of the biosynthetic pathway; the Golgi fragments and disperses through the cytoplasm (Ho et al., 1989), and early transport steps from ER to Golgi are affected (Cole et al., 1996).

Most of the current knowledge about the role of MT in organelle and vesicle motility and the involvement of motor proteins was obtained by differential interference contrast

(DIC) microscopy (Allen et al., 1982; Koonce and Schliwa, 1985; Kuznetsov et al., 1992; Schnapp et al., 1985; Travis et al., 1983; Vale et al., 1985). However, by DIC-microscopy organelles can be classified only by shape, size and contrast but not by cargo or destination (Schroer and Sheetz, 1991). Therefore the MT-dependence of a defined vesicular transport step, e.g. transport from the TGN to the PM, has not been demonstrated. To address the role of MT in this late transport step specifically, it would be advantageous to track individual transport vesicles derived from the TGN in living cells. In the past fluorescently labelled antibodies against the vesicular stomatitis virus (VSV) G protein were used for real time studies in living cells (Arnheiter et al., 1984; Storie et al., 1994). Similarly, NBD-ceramide was used to label the Golgi complex *in vivo* and it was proposed that post-Golgi fluorescent structures move along cytoskeletal elements (Cooper et al., 1990). Although both techniques have the potential to study the role of MT in transport of post-Golgi vesicles this was not specifically addressed.

We recently developed a system to study the transport from the TGN to the PM in real time in living cells (Kaether and

Gerdes, 1995). A secretory protein, human chromogranin B (hCgB) was fused to the green fluorescent protein (GFP; Cubitt et al., 1995; Gerdes and Kaether, 1996) and expressed in the secretory pathway of HeLa cells. GFP was converted to the fluorescent form when the biosynthetic transport was arrested at the TGN by a secretion block at 20°C. Release of the block by incubation at 37°C resulted in the formation of fluorescent post-Golgi vesicles that apparently were secreted after prolonged release. Because green fluorescence is not generated at 37°C this system allows us to follow secretion of fluorescent hCgB-GFP from the TGN after reversal of a secretion block in a pulse-chase-like manner.

Here we exploit this system in Vero cells to examine the role of MT in mediating the transport of secretory vesicles from the TGN to the PM. We show that transport of fluorescent vesicles obtained after release of a secretion block is facilitated by but not dependent on MT. Surprisingly, MT-dependent movement of vesicles appeared to be random and did not suggest that secretory vesicles are conveyed from the TGN to the PM by a direct route.

MATERIALS AND METHODS

Cell culture and transfection

Vero cells (ATCC CCL 81, kindly provided by Dr D. Soldati, ZMBH Heidelberg) were grown at 37°C, 5% CO₂ in DMEM containing 5% fetal calf serum and 2 mM glutamine. For transient transfection, calcium phosphate precipitation (Sambrook et al., 1989) was performed on cells grown 1 day to 50% confluency. For control experiments Vero cells were transfected with the hCgB-GFP cDNA in pBluescript (Stratagene). To create a stable cell line expressing hCgB-GFP Vero cells were cotransfected with *Sfi*I linearized hCgB-GFP/pCDM8 (Kaether and Gerdes, 1995) and *Sca*I linearized pMC1-Neo (Stratagene). Neo-resistant cells were selected with 0.5 mg/ml G418 (Gibco) and colonies of single clones were picked after 3-4 weeks. None of the neo-resistant clones was found to express detectable amounts of hCgB-GFP as determined by immunofluorescence. However, after incubation with butyrate known to enhance transcription of CMV-promoter controlled genes (Dorner et al., 1989), expression of hCgB-GFP was detected in 4 clones by western-blotting and fluorescence microscopy (data not shown). One clone, V7, was chosen and maintained in EMEM with 10% fetal calf serum, 2 mM glutamine and 0.5 mg/ml G418. To induce hCgB-GFP expression, cells were incubated for 21 hours in growth medium containing 2 mM sodium butyrate. 20°C secretion blocks were carried out in a waterbath placed in a 4°C room or in a 20°C incubator using growth medium with 10 mM Hepes, pH 7.4).

Antibody preparation and immunoblotting

A peptide with the sequence AAGITHGMDELYK corresponding to the C terminus of GFP (synthesized by Dr R. Frank, Heidelberg) was coupled to keyhole limpet haemocyanin (KLH, Calbiochem) using glutaraldehyde. Rabbits were immunized using standard procedures. Preimmune sera and bleeds after boosting were screened for immunoactivity against GFP using western blots of V7 cell lysates. One serum, D2, was shown to recognize specifically GFP. For immunoblotting, cell lysates (see below) were run on 7.5% SDS-PAGE mini-gels (Bio-Rad) and blotted onto nitrocellulose. Non-specific binding sites were blocked by incubation for 2 hours in blocking buffer (PBS/10% low fat milkpowder for antiserum D2, PBS/10% BSA for monoclonal antibody 67-C7-2; Rosa et al., 1992), then filters were incubated for 2 hours in blocking buffer/serum D2 or 67-C7-2. Intermediate wash steps were carried out with PBS/0.2%

Tween-20. Detection of bound antibodies was performed with HRP-coupled goat anti-rabbit and goat anti-mouse secondary antibodies (Dianova) for 30 minutes in blocking buffer followed by ECL detection (Amersham).

Fluorimetric determination of GFP-release

V7 and Vero wild-type cells grown for 1 day to subconfluency (10 cm Petri dishes) were incubated with 2 mM butyrate for 20 hours. After 2 hours at 20°C in external solution (ES), consisting of 140 mM NaCl, 5 mM KCl, 2 mM CaCl₂, 1 mM MgCl₂, 10 mM glucose, 10 mM Hepes, pH 7.4, buffer was removed and ES (37°C) was added. Cells were incubated at 37°C and ES was collected every 30 minutes. Emission spectra were recorded with an Aminco Bowman Fluorimeter using 470 nm as excitation wavelength. To measure cellular hCgB-GFP, cells were lysed by 3 cycles of freezing and thawing in hypotonic buffer (1 mM EDTA, 1 mM MgAc, 3.2 mM Na₂SO₄, 1.25 mM PMSF, 10 mg/ml leupeptin, 10 mM Hepes, pH 7.4) and spectra of high speed (100,000 g) supernatants were recorded. Protein content of the homogenates was determined using the Bio-Rad protein assay kit. All emission spectra were normalized to total cellular protein, emission spectra of duplicate samples were averaged. In a final step difference spectra were calculated by subtracting averaged emission spectra of wild-type cells from those of V7 cells. The peak values at 510 nm were used to calculate the release in a given time interval.

Immunofluorescence

TGN38 and cathepsin D immunolabelling: for TGN38 colocalization experiments V7 cells were transiently transfected with pMEP4-TGN38 (Reaves and Banting, 1994). TGN38 expression was induced with 2 µM CdCl₂ added to the butyrate medium two days after transfection. This concentration did not lead to aberrant localization of transfected TGN38 (not shown). Cells were rinsed once in PBS and fixed for 20 minutes in 4% paraformaldehyde/4% sucrose in PBS. After fixation cells were rinsed three times in PBS and quenched for 10 minutes in 50 mM NH₄Cl. After rinsing three times in PBS permeabilisation was achieved in 0.2% Triton X-100/PBS for 5 minutes. Antibody incubation (2F1.1B1 for TGN38, cathD #823 for cathepsin D, kindly provided by Drs G. Banting, Bristol, UK, and B. Hoflack, Heidelberg, respectively) was performed in PBS containing 0.2% gelatin for 20 minutes. After rinsing in PBS/0.2% gelatin, coverslips were incubated with Texas Red-coupled goat anti-mouse or rhodamine-coupled goat anti-rabbit IgG (Dianova) for 20 minutes. After rinsing in PBS, coverslips were mounted in Mowiol. For analysis of GFP-fluorescence, cells were fixed, incubated for 10 minutes in 50 mM NH₄Cl and mounted as described above.

Confocal microscopy

For confocal images a Leica TCS4D confocal system equipped with an ArKr laser and a ×63 1.4 NA PL APO objective was used. Fig. 5A-C were recorded with 1,024×1,024 pixel resolution, Fig. 5D with 512×512. Focal planes were scanned sequentially using first 488 nm excitation and LP 515 for GFP detection, and then 568 nm excitation and LP 590 for rhodamine or Texas Red detection. For each fluorescent image, scans from three consecutive layers were combined, transferred to Adobe Photoshop and printed on a Kodak XLS 8600PS photoprinter.

Transferrin uptake

V7 cells plated on LabTek chambered coverglass (Nunc) were blocked for 2 hours at 20°C in serum-free EMEM plus 10 mM Hepes, pH 7.4. During the second hour of block 50 µg/ml Texas Red-coupled transferrin (Molecular Probes) was present. To release the secretion block, the medium was replaced with 37°C Hepes-buffered EMEM containing Texas Red transferrin. Cells were observed in the LabTek chambers at the confocal microscope at room temperature (25°C). Images were recorded with 512×512 pixel resolution, open pinhole,

4-time line averaging and simultaneous excitation with 488 and 568 nm. Scanning time for each image was about 7 seconds.

Video microscopy

Vero cells transfected with hCgB-GFP or control DNA two or three days before the experiment were incubated for 1 hour at 20°C, then 15–20 minutes at 37°C in modified culture medium (DMEM, Sigma #D2902, with the addition of 10 mM Hepes, pH 7.3, 0.2% BSA, 3.5g/l glucose, 1.6g/l NaCl). For analysis in the absence of nocodazole cells were immediately transferred to the stage of a Zeiss Axiovert 135 and observed at 25°C in PBS. For analysis in the presence of nocodazole cells were placed on ice for one additional hour in a medium containing 1% DMSO and 50 µM nocodazole (Sigma) and then observed in PBS containing 1% DMSO and 50 µM nocodazole. First a short video sequence was recorded using phase contrast. Then epifluorescence was used to detect the GFP-signal (XBO75 lamp; FITC filter set with BP450-490, FT510, LP520; ×100/1.30 Plan-Neofluar objective). Intensified images (Videoscope Image Intensifier VS3-1845) were 8× averaged (Hamamatsu Argus10 Image Processor) and recorded with a Hi8 video recorder (SonyEVO-9650P). Individual frames were digitized automatically every second (Scion LG3 frame grabber card in a Power Macintosh 8100/80). Image analysis was performed using the public domain NIH Image program. A macro routine was designed which allows the tracking of individual particles interactively. Coordinates of individual particles at a given time were stored and their position was marked in a reference image, called track display.

Metabolic labelling and immunoprecipitation

Confluent, butyrate induced V7 cells (3.5 cm Petri dishes) were incubated for 30 minutes in methionine/cysteine free DMEM. Cells were then pulsed for 5 minutes with DMEM containing 100–150 µCi Met/Cys translabel (Amersham). After the pulse cells were blocked for 1 hour at 20°C in DMEM containing 10 mM Hepes, pH 7.4. To chase labelled proteins from the TGN, cells were incubated at 37°C in DMEM containing 100 µg/ml leupeptin and 10 and 2 times normal methionine and cysteine concentrations, respectively. In the case of nocodazole treatment, cells were placed on ice for 1 hour after the 20°C block in block medium containing 1% DMSO with or without 50 µM nocodazole then chased at 37°C in chase medium containing 1% DMSO without nocodazole. Chase medium was replaced every 30 minutes, spun 10 minutes at 3,000 rpm in a Eppendorf 5415C centrifuge, diluted 1:1 with medium dilution buffer (dilution buffer, see below, with 2% Triton X-100 and 0.5% deoxycholate) and incubated overnight with D2 antibody. After 2 hours chase, cells were washed in ice-cold PBS and lysed for 20 minutes in lysis buffer (10 mM Tris-HCl, pH 7.5, 150 mM NaCl, 1 mM EDTA, 1% Triton X-100, 0.5% deoxycholate, 1.25 mM PMSF, 100 µg/ml leupeptin). Lysates were centrifuged for 30 minutes at 43,000 rpm in a TLA45 rotor in a Beckmann TL100 ultracentrifuge. Supernatant was diluted 1:2 in dilution buffer (lysis buffer plus 0.5% SDS, 0.5% low fat milk powder, 1 mg/ml BSA) and incubated overnight with antibody D2. Protein-A Sepharose (Pharmacia CL-4B) was added for 2 hours at 4°C, followed by two washes in buffer A (10 mM Tris-HCl, pH 7.5, 150 mM NaCl, 2 mM EDTA, 0.2% Triton X-100), two washes in buffer B (buffer A with 500 mM NaCl) and one wash in buffer C (10 mM Tris-HCl, pH 7.5, 0.1% Triton X-100). After the addition of SDS-PAGE sample buffer, samples were boiled and loaded on a 6% SDS-PAGE gel. For detection and quantitation of radioactivity a Fuji Phosphoimager system was used.

RESULTS

A movie of real-time secretory vesicle transport can be viewed on the World Wide Web (<http://WWW.cityscape.co.uk/users/ag64/jcscont.htm>).

hCgB-GFP is expressed from a stable Vero cell line after induction with butyrate

To establish a stable cell line expressing hCgB-GFP, we transfected Vero cells with a cDNA encoding the recombinant protein and selected for neomycin-resistant clones. One clone, referred to as V7, expressed hCgB-GFP after butyrate induction (see Materials and Methods) and was used in the present study. V7 and Vero wild-type cells were incubated in the absence or presence of butyrate and analysed by western blotting using an anti-GFP serum raised against a peptide corresponding to the C terminus of GFP (Fig. 1). hCgB-GFP was detected only in cell lysates of V7 after butyrate treatment (lane 2) but not in untreated V7 (lane 1) or wild-type cells without or with butyrate induction (lanes 5 and 6, respectively). Specificity of the antibody for GFP was shown by competition with the peptide used for immunisation (lane 3). Competition with unrelated peptides did not result in loss of the signal (not shown). A band of the same molecular mass was also detected in cell lysates of butyrate treated V7 with a monoclonal antibody against hCgB (lane 4).

In V7 cells expressing hCgB-GFP no green fluorescence was observed by confocal microscopy under normal cell culture conditions at 37°C. Green fluorescence appeared after butyrate treatment in combination with a 20°C secretion block in a perinuclear Golgi-like compartment (Fig. 2, 0', arrowheads) which sometimes showed a peripheral expansion. The same treatment of Vero wild-type cells did not reveal green GFP-fluorescence (not shown). During subsequent incubation at 37°C the perinuclear GFP-signal vanished and concomitantly numerous green fluorescent particles appeared (Fig. 2, 10', 20', arrows). Note, that clustered perinuclear GFP-fluorescence loosened up with time (Fig. 2, compare signals indicated by arrowheads in 0', 10' and 20'). In cells on the same coverslip conversion of the perinuclear fluorescence to a vesicular pattern was not entirely synchronized. However in most cells a vesicular pattern was most prominent after 20 minutes of incubation at 37°C (Fig. 2, 20'). At 30 minutes after block release no perinuclear GFP-signal was observed and only a few green vesicles were visible (Fig. 2, 30', arrows). After 60 minutes, the remaining fluorescence is a background signal and also seen before the secretion block and in wt cells (not shown).

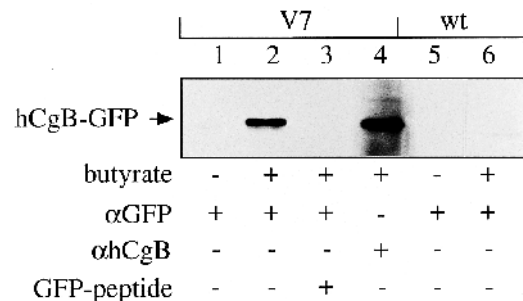


Fig. 1. Butyrate induced expression of hCgB-GFP in a stable Vero cell line. Cell lysates of a stable clone (V7) and of Vero wild-type cells (wt) with (+) or without (–) butyrate induction were analyzed by immunoblotting with GFP-antiserum (αGFP) or with hybridoma supernatant against hCgB (αhCgB). A specific band corresponding to hCgB-GFP was detected only in butyrate induced V7 cells. Specificity of αGFP was shown by addition of peptide used for immunisation (GFP-peptide).

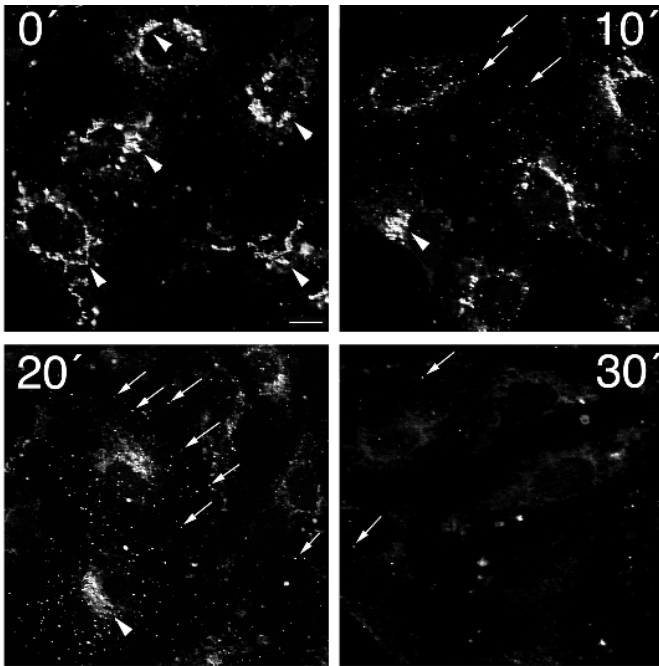


Fig. 2. Generation of green fluorescent vesicles in V7 by release of a 20°C secretion block. V7 were induced with butyrate and incubated for 2 hours at 20°C, then fixed (0') or further incubated for 10 minutes (10'), 20 minutes (20') or 30 minutes (30') at 37°C, fixed and analyzed for GFP-fluorescence by confocal microscopy. Images were visualized by simulated fluorescence process. Arrowheads, perinuclear GFP-fluorescence; arrows, GFP-labelled vesicles. Bar, 10 µm.

Complete disappearance of the fluorescent vesicles 60 minutes after the block suggested that fluorescent hCgB-GFP had been secreted, as has been described for transiently transfected HeLa cells (Kaether and Gerdes, 1995) and other fibroblast-like cell lines (C. Kaether and H.-H. Gerdes, unpublished).

Fluorescent hCgB-GFP containing vesicles are devoid of markers for the TGN and the endosomal/lysosomal compartment

We investigated whether the fluorescent particles visible after reversal of the secretion block are secretory vesicles, i.e. vesicles which transport hCgB-GFP from the TGN to the PM. First, to confirm that we observed biogenesis of TGN-derived vesicles rather than disintegration of the TGN, we compared the localisation of TGN38, a resident marker for the TGN (Luzio et al., 1990), with that of fluorescent hCgB-GFP. Because of the lack of antibodies against the TGN38 homologue in Vero cells we transiently expressed rat TGN38 in V7, and induced hCgB-GFP expression in these cells by butyrate. After a 20°C secretion block with or without subsequent release cells were fixed and immunolabelled with anti-TGN38 (Fig. 3A-C). Fig. 3A shows a transfected cell fixed directly after the block. The yellow staining juxtaposed to the nucleus indicates colocalization of TGN38 and fluorescent hCgB-GFP suggesting that the compartment in which green fluorescence first appears at 20°C is the TGN. Fig. 3B shows a transfected cell (and Fig. 3B' a magnified section of Fig. 3B) which was fixed 20 minutes after block release. In addition to

the yellow perinuclear staining numerous green particles were distributed throughout the cell (arrows in Fig. 3B'). These particles were devoid of TGN38 implying biogenesis of a vesicle with a composition different from the donor compartment. Fig. 3C shows a transfected cell 30 minutes after block reversal. The TGN38 immunostaining indicates little colocalization with green fluorescence suggesting that most of the fluorescent hCgB-GFP had left the TGN after 30 minutes at 37°C.

Disappearance of green particles 30-60 minutes after reversal of the block could reflect secretion or degradation via the endosomal/lysosomal system. To exclude the latter possibility we analyzed whether green particles colocalized with markers for lysosomes and endosomes (Fig. 3D-E). First, antibodies against cathepsin D, a marker for lysosomes, were used to stain V7 cells fixed 15 minutes after block reversal (Fig. 3D). No colocalization of green vesicles (arrows) with cathepsin D was observed. Second, to check for interaction with the endosomal pathway we labelled living V7 cells with Texas Red-transferrin and analyzed these cells ~30 minutes after block reversal by confocal microscopy *in vivo*. From this series of scans one frame is shown (Fig. 3E). Neither on this scan nor on the 14 other scans from the same series (not shown) colocalization of green particles (arrows) and Texas Red-transferrin-labelled endosomal structures was observed in the periphery of the cell. Evidently, the green fluorescent vesicles are neither lysosomes nor endosomes.

Fluorescent hCgB-GFP is secreted from V7 cells

If fluorescent hCgB-GFP is transported in secretory vesicles that fuse with the PM one should be able to recover the fluorescence in the medium and determine the kinetics of release by fluorometry. For fluorometric analysis butyrate-induced V7 cells or wild-type cells as a control were blocked for 2 hours at 20°C and chased at 37°C. Chase media were collected every 30 minutes over a 2 hour time period and emission spectra were recorded (Fig. 4A).

The spectra of the material released in the first two collection periods displayed a characteristic GFP-S65T emission spectrum as published (Heim et al., 1995) with pronounced peaks around 510 nm (Fig. 4A, 0-30', 30-60'). During later chase times much less material was released, resulting in a rather broad peak (Fig. 4A, 60-90') or no peak at all (Fig. 4A, 90-120'). During the first hour already 80% of the total GFP-fluorescence released appeared in the medium (Fig. 4B). The estimated $t_{1/2}$ of transport from the TGN to the PM was about 30 minutes.

To determine whether secretion of fluorescent hCgB-GFP is accompanied by a decrease in cellular GFP-fluorescence, spectra of cell lysates were compared from V7 cells after a 2 hour secretion block and at the end of an additional 2 hour release period at 37°C. As expected the cellular fluorescence was reduced drastically after 2 hours of release (Fig. 4C, compare 0' and 120'). The difference spectrum between the two (Fig. 4D) shows a typical GFP-spectrum as detected for the media fractions (Fig. 4A) indicating that fluorescent hCgB-GFP was secreted from the cells. In conclusion our data support the idea that hCgB-GFP is transported and secreted via a secretory vesicle.

Effect of nocodazole on the secretion of hCgB-GFP

We next tested the effect of MT disassembly on the secretion

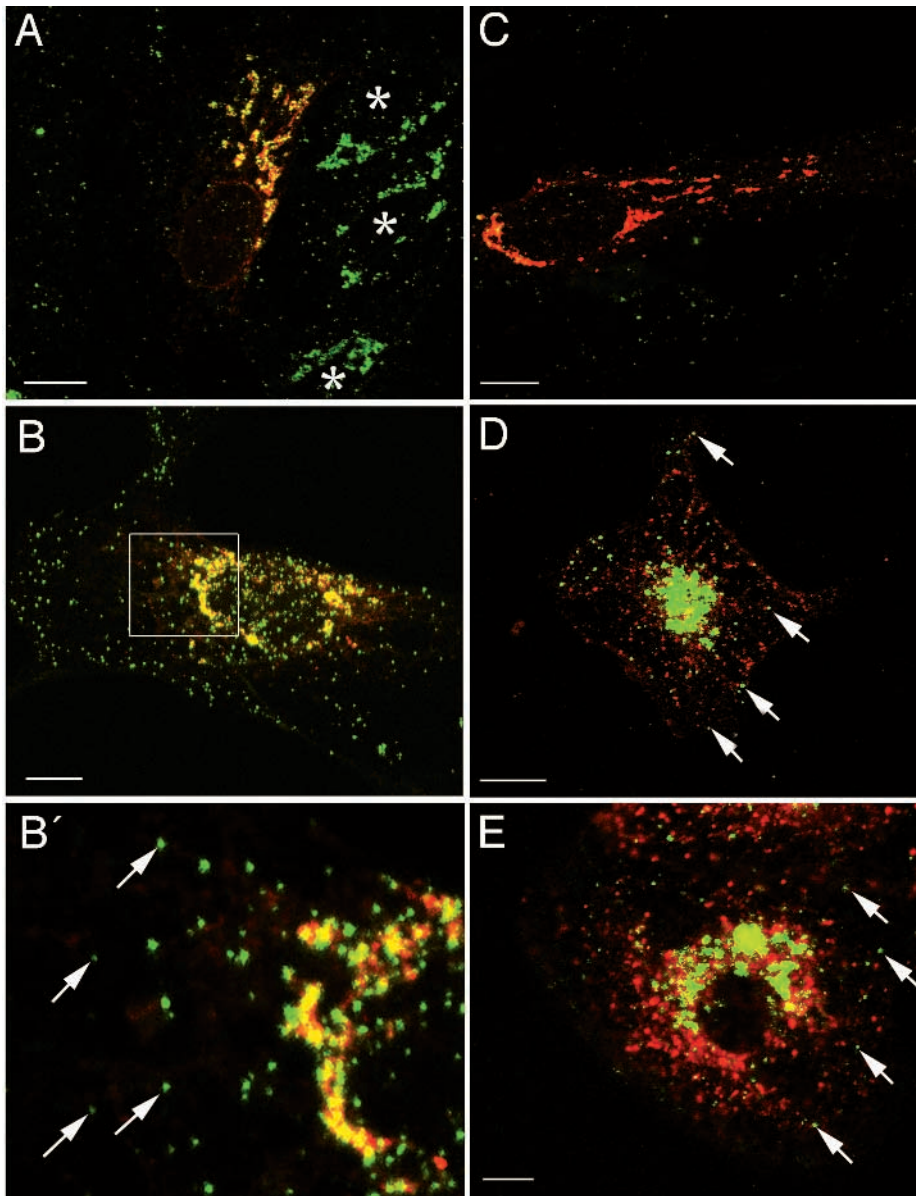


Fig. 3. Fluorescent hCgB-GFP containing vesicles do not colocalize with markers of the TGN and the endosomal/lysosomal compartment. V7 were transiently transfected with TGN38 cDNA and incubated for 2 hours at 20°C. Cells were fixed after the secretion block (A) or after an additional incubation at 37°C for 10 minutes (B) or 30 minutes (C), immunostained with antibodies against TGN38 and analyzed by confocal microscopy. (B') A higher magnification of the box in B. Note colocalization of fluorescent hCgB-GFP (green) and TGN38 (red) in a perinuclear region but not in green vesicles (arrows). (D) V7 cells incubated for 1 hour at 20°C and for 15 minutes at 37°C were fixed, immunostained with an antibody recognizing cathepsin D and analysed by confocal microscopy. Green vesicles (arrows) do not colocalize with the lysosomal marker (red). (E) Living V7 cells, incubated for 2 hours at 20°C and loaded with Texas Red-transferrin, were analysed during a subsequent reversal of the secretion block by confocal microscopy. One scan out of a series is shown. Green fluorescent vesicles (arrows) are devoid of Texas-Red transferrin-loaded endosomes. Asterisks in A indicate position of nuclei of nontransfected, rat TGN38 negative cells. Bars, 10 μ m.

of hCgB-GFP. Secretion of hCgB-GFP was monitored in V7 cells by metabolic labelling with [35 S]Met/Cys in combination with a 20°C secretion block. Pulse-chase analysis was performed in the absence or presence of nocodazole. hCgB-GFP was measured in chase media collected every 30 minutes over a 2 hour chase period and cell lysates at the end of the chase (Fig. 5A). In the absence of nocodazole the majority of 35 S-labelled hCgB-GFP was secreted during the first 30 minutes after release of the secretion block (Fig. 5B, left). The $t_{1/2}$ of secretion was estimated to 20 minutes. This value is similar to that measured by fluorometry and of α 1-antitrypsin transiently expressed in PC12 cells (C. Krömer and H.-H. Gerdes, unpublished) or COS7 (Leitinger et al., 1994) and to other constitutively secreted proteins (Futter et al., 1995; Lodish et al., 1983).

In the presence of nocodazole, the rate of secretion of hCgB-GFP was significantly lower resulting in secretion of equal amounts between 0 and 30 minutes and 30 and 60 minutes (Fig.

5A,B). The $t_{1/2}$ of hCgB secretion was estimated to 40 minutes. This value was doubled as compared to secretion in the absence of nocodazole. Furthermore, after 2 hours of chase higher amounts of hCgB-GFP remained in cell lysates of nocodazole treated cells as compared to cells in the absence of nocodazole (Fig. 5A). This finding probably reflects the fact that secretion was not completed within our observation time. Similarly, fluorescent hCgB-GFP was retained in cells for longer times after nocodazole treatment (not shown). Together these data show that secretion of hCgB-GFP is slowed down but not inhibited by disassembly of MT.

Fluorescent secretory vesicles move without a preferential direction

In vivo analysis of movement of individual fluorescent secretory vesicles was carried out by fluorescence video microscopy. Two to three days after transient transfection with hCgB-GFP Vero cells were incubated at 20°C for 1 hour to accumulate fluor-

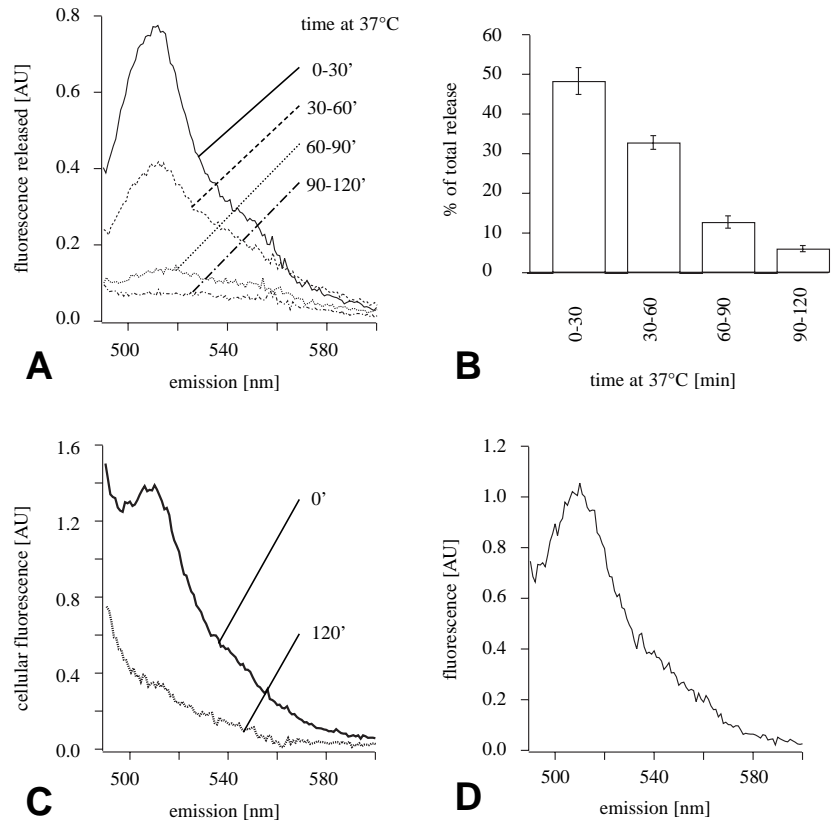


Fig. 4. Secretion kinetics of fluorescent hCgB-GFP. Butyrate induced V7 and Vero wt cells were incubated for 2 hours at 20°C followed by 2 hours of release at 37°C. Media were collected every 30 minutes during the 37°C incubation and emission spectra were recorded. (A) Difference spectra (see Materials and Methods) of chase media. (B) GFP-secretion normalized to the total release of fluorescent hCgB-GFP during the 2 hour chase (sum of the peak values at 510 nm from all four collection periods = 100%), average \pm s.e.m. of 5 independent experiments. (C) Difference spectra of cell lysates after a 2 hour secretion block (0') or after 2 hours of release at 37°C (120'). (D) GFP-spectrum calculated by subtraction of the spectrum at 120' from the spectrum at 0' in (C).

escence in the TGN, followed by 15-20 minutes incubation at 37°C to produce GFP-containing secretory vesicles. Flat and bright green cells growing solitarily or at the border of a cell colony were selected for recordings. Analysis of video sequences was done on stacks of 45 digitized images taken every second. The first image of such a stack is shown in Fig. 6A. Fluorescent vesicles showed brief periods of rapid directed movement interrupted by periods of resting. We classified the vesicles according to their motility into three categories: those showing movement over longer distances (Fig. 6C, black circles), others moving only in a limited area (Fig. 6C, white circles) and a third population (Fig. 6C, fluorescent dots without a circle) which could not be traced during the entire observation period because they left the field of view laterally, or moved into the centre of the cell where they were no longer distinguishable, or disappeared out of the plane of focus.

To characterize movements of individual vesicles, the xy-coordinates of a given particle were drawn into a reference image once a second and connected into a track display. For orienta-

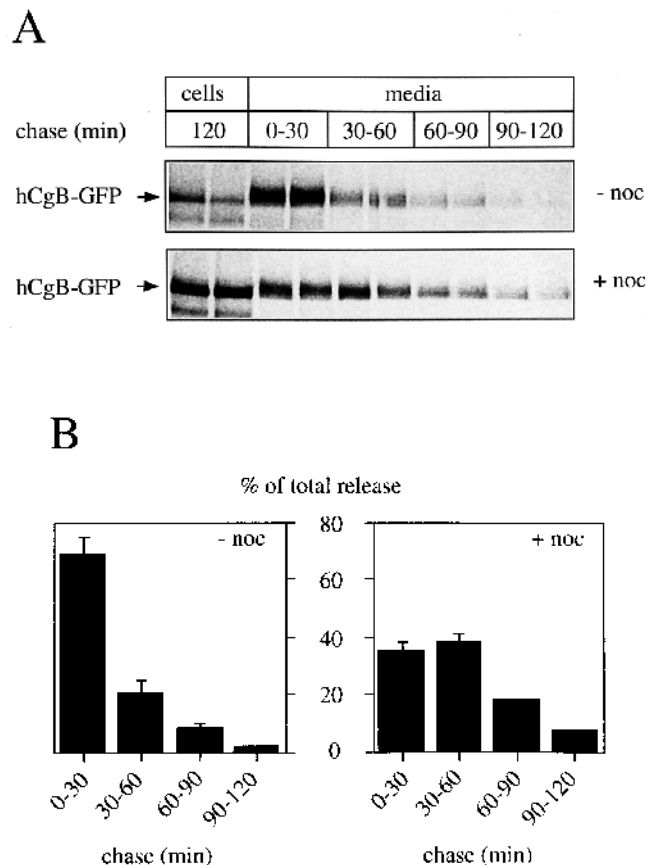


Fig. 5. Nocodazole retards secretion of [35 S]labelled hCgB-GFP. V7 were subjected to pulse-chase analysis with [35 S]Met/Cys in the absence (- noc) or presence (+ noc) of nocodazole. (A) Images of immunoprecipitated hCgB-GFP after SDS-PAGE. For both conditions two separate dishes were analysed in parallel. The media were changed every 30 minutes. Note that the lower molecular mass band in the cell lysates reflects unspecific precipitation (not displaced by GFP-peptide, data not shown). (B) Quantitation of secretion of hCgB-GFP. 100% corresponds to the amount of hCgB-GFP secreted during 2 hours of chase. The mean of two independent experiments and the variation (error bar) is shown.

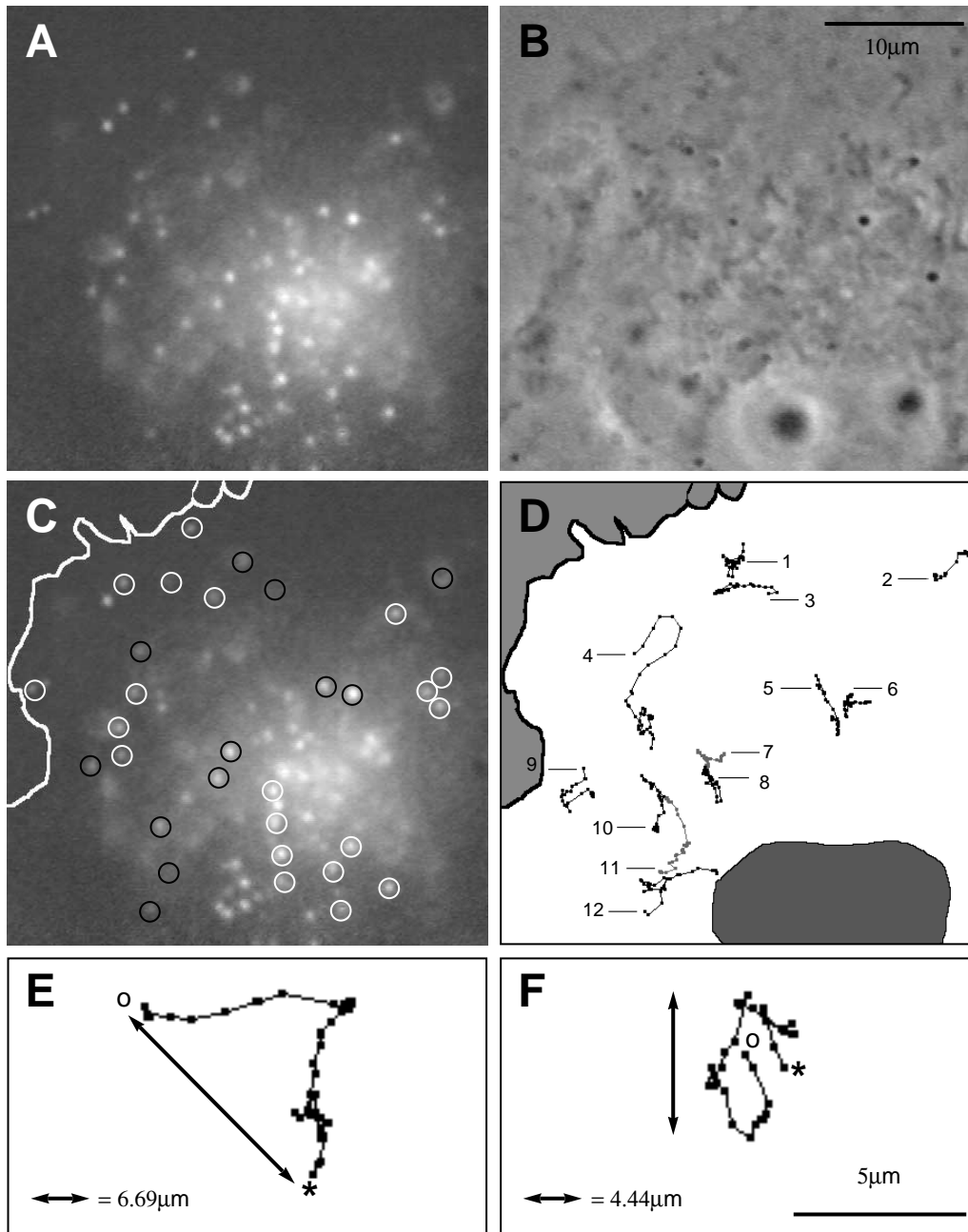


Fig. 6. Analysis of vesicle movement in single cells. hCgB-GFP transfected Vero cells were recorded after 1 hour secretion block at 20°C, followed by 15-20 minutes release at 37°C. GFP-positive vesicles were tracked individually in stacks of 45 frames digitized from videotape once per second. (A) First fluorescence image of a typical stack. (B) Phase contrast image of the same cell (recorded before the fluorescence sequence) used to trace outlines of cell and nucleus. (C) Classification of vesicles in (A); black circles indicate vesicles with a maximal displacement of $>2\ \mu\text{m}$, white circles $<2\ \mu\text{m}$, vesicles without circle could not be followed during the 45 seconds observation time. (D) Track display of vesicles with displacement $>2\ \mu\text{m}$ (black circles in C, starting points are indicated by horizontal lines). (E,F) Tracks of individual particles from other cells illustrating how the 'maximal displacement' (double-arrow) was determined. 'Asterisk' denotes the starting point, 'black circle' the end point of each track.

tion purposes, the cell of a brightfield image (Fig. 6B) was superimposed onto the fluorescence image (Fig. 6C) and onto the track display (Fig. 6D). Tracks of 12 vesicles are displayed, their starting points are marked by numbers with horizontal lines. Surprisingly, vesicle movement had no preferential direction. Vesicles moved circumferentially (Fig. 6D, 2, 3), in some instances following curvilinear tracks (Fig. 6D, 4), others moved radially towards the cell centre (Fig. 6D, 5), frequently reversed the direction of movement (Fig. 6D, 1, 3, 5, 8) or displayed more complex tracks (Fig. 6D, 10). For most vesicles, the total travel distance was much longer than the shortest distance between starting and endpoint. As a measure for the net translocation of vesicles we defined the 'maximal displacement', i.e. the distance between the two most distant points in the track display (Fig. 6E,F, double arrow). We classify movements as to 'long

distance' when the maximal displacement was larger than $2\ \mu\text{m}$ (see also Table 1). Furthermore we calculated the ratio of the travel distance of a vesicle and its maximal displacement. The value of 2.6 ± 0.1 (mean \pm s.e.m., $n=77$) indicates that a considerable amount of movement was not directed.

Individual vesicles frequently reverse their direction of movement

The surprising observation that many vesicles reversed their direction of movement led us to examine this process in more detail. An example for a vesicle that changed its direction many times is shown in Fig. 7A, white circle. For better resolution the track display of this vesicle (Fig. 7B) was divided into segments and each part was displayed separately (Fig. 7C). It shows that during ~ 90 seconds the vesicle reversed its direction 5 times

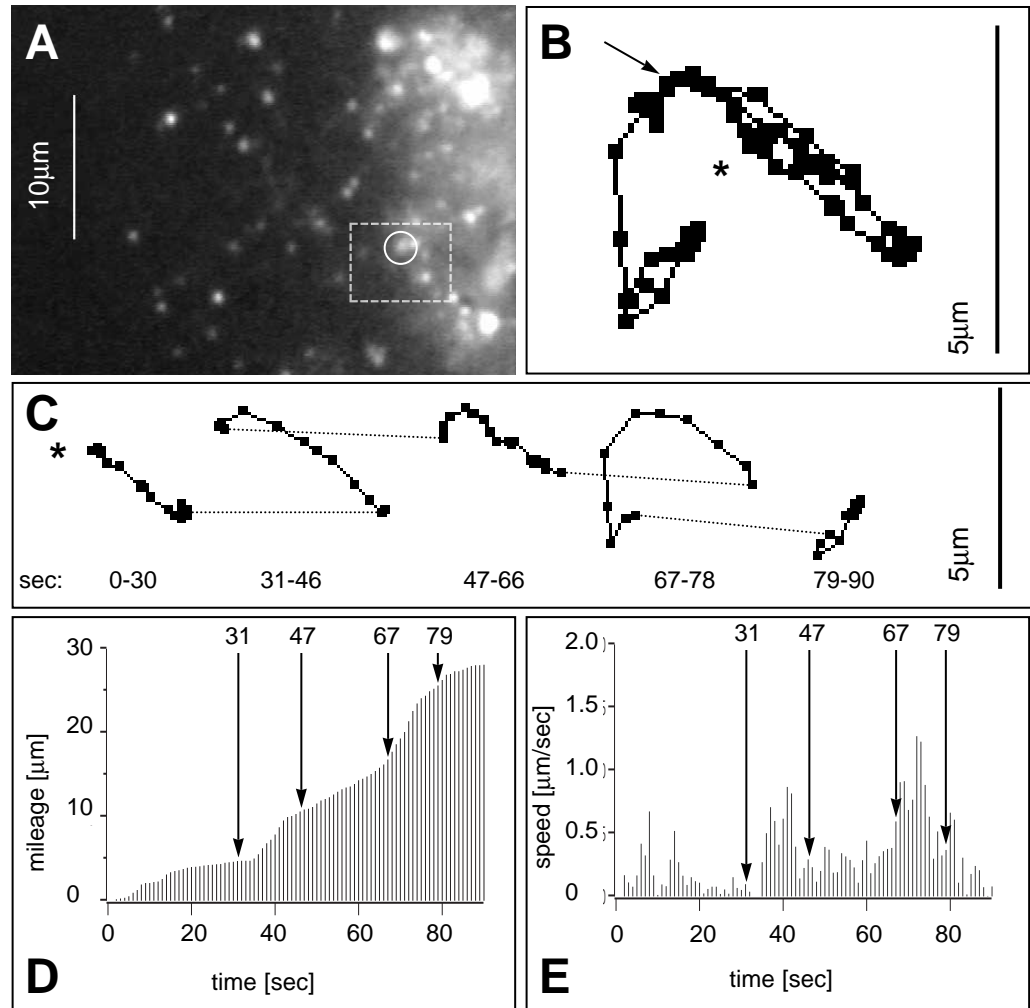


Fig. 7. Secretory vesicles reverse their direction of movement. The movement of a single vesicle was analysed for 90 seconds (A, white circle). The track of the complete observation period is shown in B; asterisk marks starting point, arrow points to a 'corridor' which was passed 4 times. The entire track was divided at the turning points and the partial tracks are displayed separately (C). Dotted lines connect the end position of each interval with the start position of the next. The travel distance of the vesicle (mileage) as a function of time is shown in D, the velocity of the vesicle at every second in E. Arrows in D and E point to the start of each interval displayed in C as a separate track.

within a 'corridor' of about $0.2 \mu\text{m}$ width (arrow in Fig. 7B) suggesting a repeated use of the same MT or bundle of MT.

To determine the frequency of reversions 100 vesicles from 8 cells with maximal displacement larger than $2 \mu\text{m}$ were analyzed. Reversion was defined as a 180° change in direction from one frame to the next. Gradual changes as seen e.g. for vesicle 4 in Fig. 6D were not considered. In addition, the vesicle had to travel back for at least $1 \mu\text{m}$ in its previous direction (vesicle 2 in Fig. 8D). Based on these criteria, 48% of the vesicles showed at least one reversion event during 45-60 seconds of observation.

Another characteristic feature of vesicle motility was the discontinuous movement of vesicles. For illustration both the integrated travel distance (referred to as mileage) and the speed of a vesicle were expressed as a function of time (Fig. 7D and E, respectively). Both graphs show how periods of little activity (e.g. seconds 16-34) alternate with periods of high activity (e.g. seconds 35-44). Note that high vesicle mobility is expressed by a steep slope in Fig. 7D and by a peak of speed in Fig. 7E. Interestingly for this and other analyzed vesicles (not shown) directional changes were paralleled by changes in velocity. Finally, the observation that the highest velocity was reached towards the end of the observation period (Fig. 7E) indicates that the translocation machinery was not impaired by photodamage.

To quantitate the maximal velocity of green fluorescent

vesicles we determined the travel distance of individual vesicles per second over an observation period of 45 seconds. Altogether 77 vesicles (in 8 cells) with a displacement larger than $2 \mu\text{m}$ were analyzed. The obtained value of $1.033 \pm 0.035 \mu\text{m}/\text{second}$ (mean \pm s.e.m.) is in the range of those found by DIC-microscopy for a mixture of endo/exocytic vesicles (Hamm-Alvarez et al., 1993).

Movement of secretory vesicles is microtubule-dependent

The observed movement of secretory vesicles along tracks together with the finding that secretion of hCgB-GFP was retarded after nocodazole treatment prompted us to analyze the MT-dependence of secretory vesicle translocation *in vivo*. For videomicroscopy, green fluorescent vesicles were generated in transiently transfected Vero cells by a 1 hour secretion block at 20°C followed by a 15 minutes release of the block at 37°C . This release time was chosen because after 15 minutes of release at least 50% of the fluorescent hCgB-GFP had left the TGN in secretory vesicles. Subsequently, MT were depolymerized with $50 \mu\text{M}$ nocodazole for 1 hour on ice. Efficient depolymerization under these conditions as well as complete repolymerization of MT after removal of the drug within 30 minutes at 37°C was confirmed by immunofluorescence with a tubulin antibody (not shown). Videomicroscopy was carried

Table 1. Movement of vesicles is reduced in the presence of nocodazole

	Control	+ Nocodazole
Max. displacement <2 μm	36.5 \pm 6.9%	86.2 \pm 8.2%
Max. displacement >2 μm	38.5 \pm 4.6%	8.9 \pm 4.6%
Lost from view	25.0 \pm 4.5%	4.9 \pm 3.7%
Number of cells	8	5
Total number of particles	268	146

The behaviour of all discernible vesicles in a given cell (Fig. 6C) was analyzed during a fixed time interval of 45 seconds. The proportion of vesicles per cell falling into one of three categories was determined, then the percentage values in each category were averaged (means \pm s.e.m.).

out in the presence of nocodazole at room temperature and movement of individual vesicles was analyzed as described for control cells. Although it is known that the Golgi complex disintegrates after MT-disassembly, the 15 minute block release before nocodazole treatment ensured that the majority of fluorescent structures were secretory vesicles.

Classification of all GFP-positive vesicles into three categories according to their displacement (Table 1) shows that after nocodazole treatment: (i) the relative proportion of vesicles with maximal displacement of less than 2 μm was doubled as compared to control cells; (ii) the relative proportion of vesicles with maximal displacement more than 2 μm

was reduced to one fourth as compared to control cells; and (iii) the relative proportion of vesicles which were lost from view was strongly diminished.

To compare movement of individual secretory vesicles from cells with or without nocodazole, the 10 vesicles per cell with the largest displacement were selected for each condition (Fig. 8A,B, white circles) and the corresponding tracks were analysed. Tracks in nocodazole-treated cells (Fig. 8C) were found to be much shorter than in control cells (Fig. 8D). We quantitated the maximal displacement of vesicles under both conditions. Most strikingly, the peak obtained for the maximal displacement in the presence of nocodazole was shifted to 4 times shorter values as compared to control cells (Fig. 9). These data strongly suggest an essential role for MT in the transport of hCgB-GFP containing secretory vesicles. Interestingly, the few vesicles in nocodazole-treated cells with displacements comparable to control cells reached values for the maximal velocities similar to those measured in untreated cells (not shown). Therefore we assume that some MT were resistant to nocodazole and allowed normal transport even in the presence of the drug.

DISCUSSION

Tracking of secretory vesicles

In the present study we have used a GFP-tagged secretory protein to analyse in living cells vesicular transport from the TGN to the

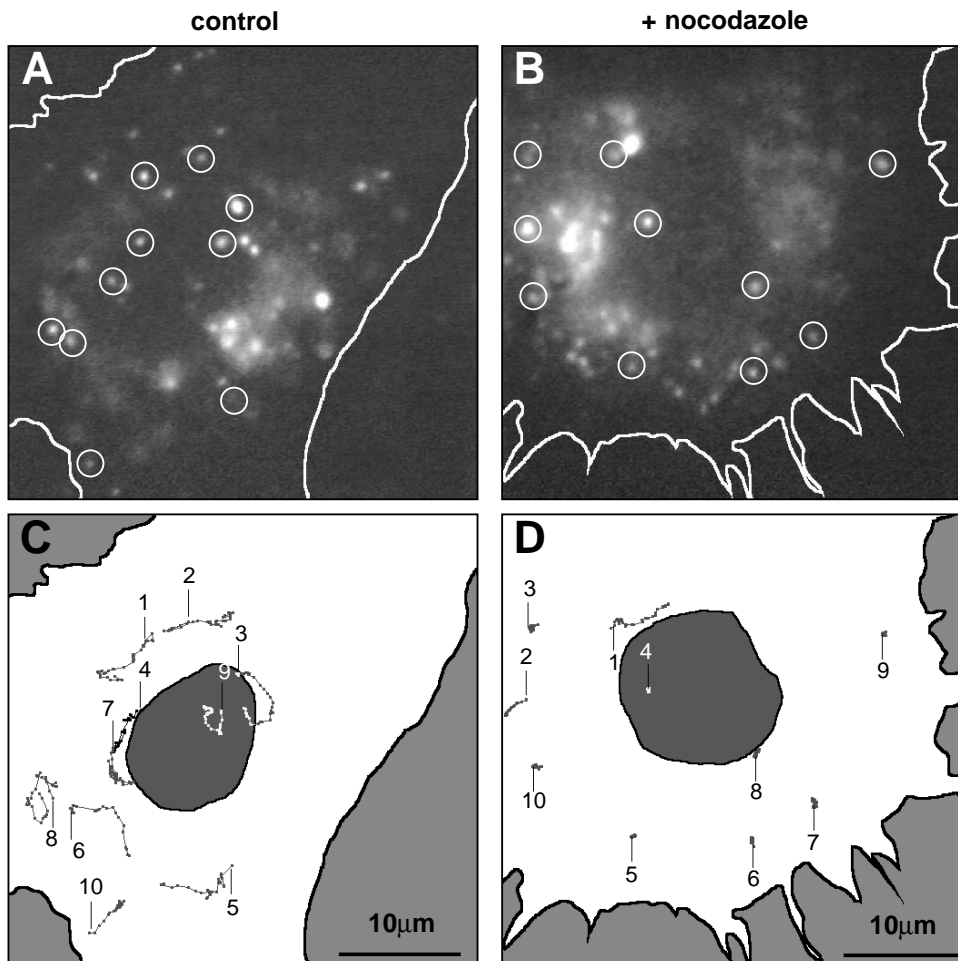


Fig. 8. Motility of secretory vesicles is strongly reduced after disassembly of MT. hCgB-GFP transfected Vero cells blocked for 1 hour at 20°C and chased for 15–20 minutes at 37°C (A,C) or blocked, chased and nocodazole-treated (B,D), were recorded and images processed as described. (A,B) Fluorescence images of typical cells, the 10 particles with the largest displacement are indicated by white circles. (C,D) Track display of vesicles depicted in A and B, respectively. Individual vesicles are numbered, the vertical lines indicate the starting point of the corresponding track. Cells are shown in white, nuclei in dark gray.

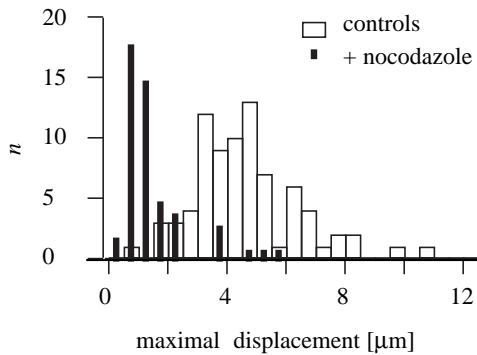


Fig. 9. Maximal displacement is reduced in the presence of nocodazole. From every cell the 10 vesicles with the largest displacement were analyzed ($n=80$ for controls, $n=50$ for nocodazole-treated cells). The 'maximal displacement' was determined from the track display. The bar graph shows the number of vesicles (n) as a function of 'maximal displacement'.

PM. The use of a GFP-mutant which is not converted to its fluorescent form at 37°C enabled us to follow TGN-derived, GFP-labelled vesicles in a pulse-chase-like manner after reversal of a temperature-dependent secretion block. Transport vesicles formed in the early secretory pathway during release of the block do not interfere with our analysis because these vesicles do not contain fluorescent hCgB-GFP. The following results convinced us that GFP-labelled vesicles obtained under these conditions are secretory vesicles: (i) metabolically labelled and fluorescent hCgB-GFP are secreted; (ii) the time course of appearance/disappearance of fluorescent vesicles matches with the secretion kinetics, and (iii) GFP-fluorescent vesicles lack detectable amounts of a resident marker of the donor compartment, TGN, and of markers of the endosomal/lysosomal system. Furthermore the secretion kinetics obtained by metabolic labelling suggest that hCgB-GFP is secreted by a constitutive secretory vesicle.

Secretory vesicles move in a MT-dependent manner

We demonstrated by videomicroscopy that green fluorescent secretory vesicles showed brief periods of directed movement. Surprisingly, they moved in a stochastic manner and frequently reversed their direction, sometimes using apparently the same track. In agreement with our observations a saltatory and random movement of post-TGN vesicles was found when fluorescent antibodies against the VSV G protein were injected into living infected cells (Arnheiter et al., 1984) or when NDB-ceramide was used as a fluorescent vital stain to label the TGN (Cooper et al., 1990). Moreover, in the latter study it was proposed that small fluorescent particles moved along cytoskeletal tracks. We made similar observations for GFP-labelled secretory vesicles and showed in addition by nocodazole treatment that the observed movement depended on an intact MT network. In accordance with our finding, cessation of virtually all directed movements of small vesicles (presumably a mixture of exo- and endocytic vesicles) was observed by DIC-microscopy of CV-1 cells when nocodazole was applied (Hamm-Alvarez et al., 1993).

Comparison with previous studies on the effect of MT-disassembly on secretion

In unpolarized cells no significant effect on the process of

transport from the TGN to the PM was found for secretory proteins (for references see Rogalski et al., 1984). This finding does not contradict our result that secretion of hCgB-GFP was halved within the first hour of chase. Rather, the long chase times used in many studies, e.g. 4 hours (Virtanen and Vartio, 1986), may not have allowed us to detect retardation of secretion. Delivery of membrane proteins from the TGN to the PM was found to be insensitive to microtubule-depolymerising drugs (Rogalski et al., 1984; Stults et al., 1989). These studies are not directly comparable to our data obtained with a secretory protein, because membrane proteins might be transported in different carriers (Boll et al., 1991; Saucan and Palade, 1992). Likewise numerous studies on the MT-dependence of secretion in polarized cells (for reviews see Cole and Lippincott-Schwartz, 1995; Schroer and Sheetz, 1991) may not be comparable due to the different MT-organisation of polarized cells (Mays et al., 1994).

Nocodazole diminished the rate of secretion less than the movement of vesicles

We found that the secretion rate of hCgB-GFP was reduced by 50% upon nocodazole treatment while the maximal displacement of vesicles dropped 4-fold under the same experimental conditions. Based on these findings we suggest that vesicular transport in the presence of nocodazole was accomplished at rates not detectable during our video recordings. Because it is difficult to reconcile vesicle movement via diffusion due to the viscosity of the cytoplasm (Luby-Phelps et al., 1987) and the extensive meshwork of the cytoskeleton, we rather assume that other transport mechanisms (Fath and Burgess, 1993; Wang and Goldman, 1978) may have contributed to vesicle translocation at low velocities.

'Trial and error' model for vesicle delivery

When we started our experiments we expected to see secretory vesicles attached to a MT-track, moving with a plus end directed motor protein to the periphery and eventually fusing with the PM. Instead, we observed that secretory vesicles moved along tracks but frequently changed their direction resulting in a seemingly random movement. Evidently, secretory vesicles are not delivered straight from the TGN to the PM.

As an explanation for the observed stochastic and energy consuming movement we propose a 'trial and error mechanism' for delivery of a vesicle to its destination. According to this model vesicles are transported fast but on random tracks simply trying any direction to increase the probability for finding their target membrane (see also Vale et al., 1992). This is consistent with the idea that the vesicle's address code specifies only the target membrane (Rothman, 1994) and not the route by which it is reached.

What could be the molecular basis for a 'trial and error' mechanism? Our observations suggest the involvement of kinesin- and dynein-like motor proteins. Recently, it was proposed that axonal vesicles are equipped with both motor proteins and that the kinesin motor is dominant, overriding the minus-end motor (Muresan et al., 1996). The absence or presence of kinesin therefore would determine the direction of movement of vesicles and back and forth movement, as we observed for secretory vesicles, would suggest a fast association/dissociation rate of kinesin.

Perspectives

The approach presented in this study for analyzing post-Golgi traffic opens up the possibility to further elucidate biogenesis and transport of TGN-derived carrier vesicles. In particular, the role of MT in the formation of these vesicles and the regulation of the motor proteins involved in their transport can be addressed *in vivo*. Moreover it would be interesting to tag proteins destined for late endosomes/lysosomes with GFP and to follow transport routes to these organelles. It can be expected that real time studies of vesicular traffic will extend the knowledge obtained from biochemical studies and will contribute to a better understanding of dynamic processes in the cell.

C. Kaether and H.-H. Gerdes gratefully acknowledge Dr W. B. Huttner for his continuous support. We also thank Dr G. Banting for providing cDNA encoding ratTGN38 and antibodies against TGN38, Dr B. Hoflack for antibodies against cathepsin D, Dr W. Knebel (Leica) for advice in confocal microscopy and Dr M. Hannah for critical comments on the manuscript. C. Kaether is supported by the Graduiertenkolleg 'Molekulare und Zelluläre Neurobiologie', H.-H. Gerdes is a recipient of a grant from the Deutsche Forschungsgemeinschaft (SFB 317/C7).

REFERENCES

- Allen, R. D., Metzuzals, J., Tasaki, I., Brady, S. T. and Gilbert, S. P. (1982). Fast axonal transport in squid giant axon. *Science* **218**, 1127-1129.
- Arnheiter, H., Dubois-Dalcq, M. and Lazzarini, R. A. (1984). Direct visualization of protein transport and processing in the living cell by microinjection of specific antibodies. *Cell* **39**, 99-109.
- Boll, W., Partin, J. S., Katz, A. I., Caplan, M. J. and Jamieson, J. D. (1991). Distinct pathways for basolateral targeting of membrane and secretory proteins in polarized epithelial cells. *Proc. Nat. Acad. Sci. USA* **88**, 8592-8596.
- Cole, N. B. and Lippincott-Schwartz, J. (1995). Organization of organelles and membrane traffic by microtubules. *Curr. Opin. Cell Biol.* **7**, 55-64.
- Cole, N. B., Sciaky, N., Marotta, A., Song, J. and Lippincott-Schwartz, J. (1996). Golgi dispersal during microtubule disruption: regeneration of Golgi stacks at peripheral endoplasmic reticulum exit sites. *Mol. Cell Biol.* **7**, 631-650.
- Cooper, M. S., Cornell-Bell, A. H., Chernjavsky, A., Dani, J. W. and Smith, S. J. (1990). Tubulovesicular processes emerge from *trans*-Golgi cisternae, extend along microtubules, and interlink adjacent *trans*-Golgi elements into a reticulum. *Cell* **61**, 135-145.
- Cubitt, A. B., Heim, R., Adams, S. R., Boyd, A. E., Gross, L. A. and Tsien, R. Y. (1995). Understanding, improving and using green fluorescent proteins. *Trends Biochem. Sci.* **20**, 448-455.
- Dorner, A. J., Wasley, L. C. and Kaufman, R. J. (1989). Increased synthesis of secreted proteins induces expression of glucose-related proteins in butyrate-treated Chinese hamster ovary cells. *J. Biol. Chem.* **264**, 20602-20607.
- Fath, K. R. and Burgess, D. R. (1993). Golgi-derived vesicles from developing epithelial cells bind actin filaments and possess myosin-I as a cytoplasmically oriented peripheral membrane protein. *J. Cell Biol.* **120**, 117-127.
- Futter, C. E., Connolly, C. N., Cutler, D. F. and Hopkins, C. R. (1995). Newly synthesized transferrin receptors can be detected in the endosome before they appear on the cell surface. *J. Biol. Chem.* **270**, 10999-11003.
- Gerdes, H.-H. and Kaether, C. (1996). Green fluorescent protein: applications in cell biology. *FEBS Lett.* **389**, 44-47.
- Hammer-Alvarez, S. F., Kim, P. Y. and Sheetz, M. P. (1993). Regulation of vesicle transport in CV-1 cells and extracts. *J. Cell Sci.* **106**, 955-966.
- Heim, R., Cubitt, A. B. and Tsien, R. Y. (1995). Improved green fluorescence. *Nature* **373**, 663-664.
- Ho, W. C., Allan, V. J., van Meer, G., Berger, E. G. and Kreis, T. E. (1989). Reclustering of scattered Golgi elements occurs along microtubules. *Eur. J. Cell Biol.* **48**, 250-263.
- Kaether, C. and Gerdes, H.-H. (1995). Visualization of protein transport along the secretory pathway using green fluorescent protein. *FEBS Lett.* **369**, 267-271.
- Kelly, R. B. (1990). Microtubules, membrane traffic, and cell organization. *Cell* **61**, 5-7.
- Koonce, M. P. and Schliwa, M. (1985). Bidirectional organelle transport can occur in cell processes that contain single microtubules. *J. Cell Biol.* **100**, 322-326.
- Kuznetsov, S. A., Langford, G. M. and Weiss, D. G. (1992). Actin-dependent organelle movement in squid axoplasm. *Nature* **356**, 722-725.
- Leitinger, B., Brown, J. L. and Spiess, M. (1994). Tagging secretory and membrane proteins with a tyrosine sulfation site. *J. Biol. Chem.* **269**, 8115-8121.
- Lodish, H. F., Kong, N., Snider, M. and Strous, G. J. A. (1983). Hepatoma secretory proteins migrate from rough endoplasmic reticulum to Golgi at characteristic rates. *Nature* **304**, 80-83.
- Luby-Phelps, K., Castle, P. E., Taylor, D. L. and Lanni, F. (1987). Hindered diffusion of inert tracer particles in the cytoplasm of mouse 3T3 cells. *Proc. Nat. Acad. Sci. USA* **84**, 4910-4913.
- Luzio, J. P., Brake, B., Banting, G., Howell, K. E., Braghetta, P. and Stanley, K. K. (1990). Identification, sequencing and expression of an integral membrane protein of the trans-Golgi network (TGN38). *Biochem. J.* **270**, 97-102.
- Mays, R. W., Beck, K. A. and Nelson, W. J. (1994). Organisation and function of the cytoskeleton in polarized epithelial cells: a component of the protein sorting machinery. *Curr. Opin. Cell Biol.* **6**, 16-24.
- Muresan, V., Godek, C. P., Reese, T. S. and Schnapp, B. J. (1996). Plus-end motors override minus-end motors during transport of squid axon vesicles on microtubules. *J. Cell Biol.* **135**, 383-397.
- Reaves, B. and Banting, G. (1994). Overexpression of TGN38/41 leads to mislocalisation of γ -adaptin. *FEBS Lett.* **351**, 448-456.
- Rogalski, A. A., Bergman, J. E. and Singer, S. J. (1984). Effect of microtubule assembly status on the intracellular processing and surface expression of an integral protein of the plasma membrane. *J. Cell Biol.* **99**, 1101-1109.
- Rosa, P., Bassetti, M., Weiss, U. and Huttner, W. B. (1992). Widespread occurrence of chromogranins/secretogranins in the matrix of secretory granules of endocrinologically silent pituitary adenomas. *J. Histochem. Cytochem.* **40**, 523-533.
- Rothman, J. E. (1994). Mechanisms of intracellular protein transport. *Nature* **372**, 55-63.
- Sambrook, J., Fritsch, E. F. and Maniatis, T. (1989). *Molecular Cloning: a Laboratory Manual*. Cold Spring Harbor Laboratory Press, Cold Spring Harbor, NY.
- Saucan, L. and Palade, G. E. (1992). Differential colchicine effects on the transport of membrane and secretory proteins in rat hepatocytes *in vivo*: bipolar secretion of albumin. *Hepatology* **15**, 714-721.
- Schnapp, B. J., Vale, R. D., Sheetz, M. P. and Reese, T. S. (1985). Single microtubules from squid axoplasm support bidirectional movement of organelles. *Cell* **40**, 455-462.
- Schroer, T. A. and Sheetz, M. P. (1991). Functions of microtubule-based motors. *Annu. Rev. Physiol.* **53**, 629-652.
- Storie, B., Pepperkok, R., Stelzer, E. H. K. and Kreis, T. E. (1994). The intracellular mobility of a viral membrane glycoprotein measured by confocal microscope fluorescence recovery after photobleaching. *J. Cell Sci.* **107**, 1309-1319.
- Stults, N. L., Fechheimer, M. and Cummings, R. D. (1989). Relationship between Golgi architecture and glycoprotein biosynthesis and transport in Chinese hamster ovary cells. *J. Biol. Chem.* **264**, 19956-19966.
- Travis, J. L., Kenealy, J. F. and Allen, R. D. (1983). Studies on the motility of the foraminifera. II. The dynamic microtubular cytoskeleton of the reticulopodial network of *Allogromia laticollaris*. *J. Cell Biol.* **97**, 1668-1676.
- Vale, R. D., Schnapp, B. J., Reese, T. S. and Sheetz, M. P. (1985). Movement of organelles along filaments dissociated from the axoplasm of the squid giant axon. *Cell* **40**, 449-454.
- Vale, R. D., Malik, F. and Brown, D. (1992). Directional instability of microtubule transport in the presence of kinesin and dynein, two opposite polarity motor proteins. *J. Cell Biol.* **119**, 1589-1596.
- Virtanen, I. and Vartiainen, T. (1986). Microtubule disruption does not prevent intracellular transport and secretory processes of cultured fibroblasts. *Eur. J. Cell Biol.* **42**, 281-287.
- Wang, E. and Goldman, R. D. (1978). Functions of cytoplasmic fibers in intracellular movements in BHK-21 cells. *J. Cell Biol.* **79**, 708-726.